Imaginary part of the ^{9}C -^{9}Be single-folded optical potential

A. Bonaccorso,[1,*] F. Carstoiu,[2] and R. J. Charity[3]
[1]*INFN, Sezione di Pisa, Largo B. Pontecorvo 3, 56127 Pisa, Italy*
[2]*Institute of Atomic Physics, PO Box MG-6, Bucharest, Romania*
[3]*Department of Chemistry, Washington University, St. Louis, Missouri 63130, USA*
(Received 5 July 2016; published 7 September 2016)

In a recent publication we have argued that using two very successful n-^{9}Be optical potentials [A. Bonaccorso and R. J. Charity, Phys. Rev. C **89**, 024619 (2014)] and microscopic projectile densities, it is possible to build a single-folded (light-) nucleus-^{9}Be imaginary optical potential which is more accurate than a double-folded optical potential. By comparing to experimental reaction cross sections, we showed for ^{8}B, ^{8}Li, and ^{8}C projectiles, that a very good agreement between theory and data could be obtained with such a "bare" potential, at all but the lowest energies where a small semimicroscopic surface term was added to the single-folded potential to take into account projectile breakup. In this paper we extend this study to the case of ^{9}C projectiles and assess the sensitivity to the projectile density used. We then obtained the modulus of the nucleus-nucleus S matrix and parametrize it in terms of a strong-absorption radius R_s and finally extracted the phenomenological energy dependence of this radius. This approach could be the basis for a systematic study of optical potentials for light exotic nuclei scattering on light targets and/or parametrizations of the S matrix. Furthermore our study will serve to make a quantitative assessment of the description of the core-target part of knockout reactions, in particular their localization in terms of impact parameters.

DOI: 10.1103/PhysRevC.94.034604

I. INTRODUCTION

Light exotic nuclei have been studied extensively in the last 30 years and their structure was first enlightened from measurements of the total reaction cross sections analyzed in terms of the Glauber model [1]. This lead automatically to calculations of imaginary parts of the nucleus-nucleus optical potential in the folding model. Such a procedure, although very simple, is questionable because the folding model is first order in the nucleon-nucleon interaction, while the Feshbach imaginary potential is second order for a real nucleon-nucleon interaction. Furthermore for light projectiles on light targets, the optical model itself has to be handled with great care.

Recently [2] we have argued that using two very successful n-^{9}Be optical potentials [3] and microscopic projectile densities, such as the *ab initio* VMC (Variational Monte Carlo) [4,5], it is possible to build a single-folded (light-) nucleus-^{9}Be optical potential which is more accurate than a double-folded optical potential thus overcoming the difficulties discussed above. This is because the n-^{9}Be optical potentials have strong surface terms in common for both the real and the imaginary parts which represent deformation effects, giant resonance excitations, and the breakup channels of the target. On the other hand, *ab initio* VMC [4,5] or other microscopic densities for the projectile would not contain enough information to reproduce the breakup channels of the projectile. By comparing to experimental reaction cross sections, we showed in Ref. [2], that for the cases of ^{8}B, ^{8}Li, and ^{8}C projectiles, a very good agreement between theory and data could be obtained by adding, at the lower energies, a small surface term to the single-folded potential. In this paper we extend the study to the case of ^{9}C projectiles, compare to results obtained with the JLM potential [6–9], and assess the sensitivity of the result to the projectile density used. We obtain then the nucleus-nucleus S matrix, S_{NN}, and parametrize $|S_{NN}|^2$ in terms of a strong-absorption radius [c.f. Eq. (11)] and finally extract the phenomenological energy dependence of the parameter R_s. Our results could have interesting implications in knockout formalisms as well.

^{9}Be is one of the ideal black-disk targets because it does not have bound excited states and for this reason it has been chosen in the majority of cases in which breakup of the projectile or total reaction cross sections have been studied. It has strong breakup channels itself but indeed these are taken into account by the n-^{9}Be optical potentials [3] we have developed which are able to reproduce at the same time the total, elastic, reaction cross sections and all available elastic scattering angular distributions.

On the other hand, one of the motivations for paying particular attention to ^{9}C as a projectile, is in nuclear astrophysics [10]: the current knowledge of the rate of the $^{8}\mathrm{B}\,(p,\gamma)^{9}\mathrm{C}$ reaction in stellar conditions is contradictory at best and there is little hope to resolve this, now or in in the future, by means other than by indirect methods such as for example the ANC from the breakup $^{9}\mathrm{C} \rightarrow {}^{8}\mathrm{B} + p$. This reaction gives a possible path to the hot pp chain pp-IV at high temperatures and away from it toward a rapid α process at high temperatures and densities and therefore it is important in understanding nucleosynthesis in supermassive hot stars in the early universe, including the possible of bypassing the 3α process. The correct description of the breakup reaction implies a precise knowledge of the various optical potentials and the corresponding S matrices at intermediate energies in the ^{9}C-target, ^{8}B-target, and p-target channels.

Another motivation is two-proton radioactivity which has been studied recently by the HiRA collaboration [11–14]. They have applied nucleon removal to situations in which the

*Corresponding author: bonac@df.unipi.it

remaining "core" is beyond the drip line, such as ^{8}C, unbound by one or more protons, and whose excitation-energy spectrum can be obtained by the invariant-mass method. By gating on the ground-state peak, "core" parallel-momentum distributions and total knockout cross sections have been obtained similar to previous studies with well-bound "cores". In addition for each projectile, knock out to final bound states has also been obtained in several cases.

II. NUCLEUS-NUCLEUS OPTICAL POTENTIAL

We remind the reader here of some well-known formulas that we need to refer to in the following.

The Glauber reaction cross section is given by

$$\sigma_R = 2\pi \int_0^\infty bdb(1 - |S_{NN}(\mathbf{b})|^2), \tag{1}$$

where

$$|S_{NN}(\mathbf{b})|^2 = e^{2\chi_I(b)} \tag{2}$$

is the probability that the nucleus-nucleus (NN) scattering is elastic for a given impact parameter $\mathbf{b}$.

The imaginary part of the eikonal phase shift is given by

$$\begin{aligned}\chi_I(\mathbf{b}) &= \frac{1}{\hbar v}\int dz W^{NN}(\mathbf{b},z) \\ &= \frac{1}{\hbar v}\int dz \int d\mathbf{r_1} W^{nN}(\mathbf{r_1}-\mathbf{r})\rho(\mathbf{r_1}),\end{aligned} \tag{3}$$

where W^{NN} is negative defined as

$$W^{NN}(\mathbf{r}) = \int d\mathbf{b_1} W^{nN}(\mathbf{b_1}-\mathbf{b},z)\int dz_1 \rho(\mathbf{b_1},z_1). \tag{4}$$

This quantity is the imaginary part of the single-folded optical potential given in terms of a nucleon-nucleus (nN) optical potential $W^{nN}(\mathbf{r})$ and the matter density $\rho(\mathbf{b_1},z_1)$ of the other nucleus. In the single-folding method, $W^{nN}(\mathbf{r})$ can be the imaginary part of a phenomenological nucleon-target potential such as the (DOM) or the (AB) potentials of Ref. [3]. In the double-folding method, W^{NN} is obtained from the microscopic densities $\rho_{p,t}(\mathbf{r})$ for the projectile and target, respectively, and an energy-dependent nucleon-nucleon (nn) cross section σ_{nn}, i.e.,

$$W^{NN}(\mathbf{r}) = -\frac{1}{2}\hbar v\sigma_{nn}\int d\mathbf{b_1}\rho_p(\mathbf{b_1}-\mathbf{b},z)\int dz_1\rho_t(\mathbf{b_1},z_1). \tag{5}$$

Also

$$W^{nN}(\mathbf{r}) = -\tfrac{1}{2}\hbar v\sigma_{nn}\rho_t(\mathbf{r}) \tag{6}$$

is a single-folded zero-range n-target imaginary potential and v is the nucleon-target velocity of relative motion. The W^{nN} potential of Eq. (6) has the same range as the target density because σ_{nn} is a simple scaling factor. With the potential Eq. (5), the phase shift becomes

$$\chi_I(\mathbf{b}) = -\frac{1}{2}\sigma_{nn}\int d\mathbf{b_1}\int dz\rho_p(\mathbf{b_1}-\mathbf{b},z)\int dz_1\rho_t(\mathbf{b_1},z_1). \tag{7}$$

A finite-range potential can also be defined as

$$W_I^{NN}(\mathbf{r}) = -\frac{1}{2}\hbar v\int d\mathbf{r_1}d\mathbf{r_2}\rho_p(\mathbf{r_1})\rho_t(\mathbf{r_2})v_{nn}(\mathbf{r_1}+\mathbf{r}-\mathbf{r_2}), \tag{8}$$

where v_{nn} can be a zero-range or a finite-range nucleon-nucleon interaction such as Gogny [15] or M3Y [16] or a phenomenological form. In particular a Gogny interaction [15] contains a pseudo-zero-range power density dependent term. Equation (8) can give reasonable potentials, however, the imaginary parts need to be renormalized most of the time.

The previous equations can be generalized in a obvious way in order to distinguish between the proton and neutron densities and the proton-neutron and proton-proton cross sections, using: $\rho_p = \rho^n{}_p + \rho^p{}_p$, and $W^{nN}(\mathbf{r}) = -\frac{1}{2}\hbar v(\sigma_{np}\rho^p{}_t(\mathbf{r}) + \sigma_{pp}\rho^n{}_t(\mathbf{r}))$.

In this paper we will: i) compare the characteristics of the imaginary potentials calculated from Eq. (4) using the potentials of Ref. [3], from Eq. (5) using microscopic densities, and with the JLM potential; ii) compare the respective S matrices from Eq. (2) and obtain the strong-absorption radii R_s defined as $|S_{NN}(R_s)|^2 = \frac{1}{2}$. We will also compare integrands of Eq. (1) to study "localization" effects on the reaction cross section; iii) calculate the reaction cross sections obtained from Eq. (1) using the single-folded potential Eq. (4) and the double-folded potential Eq. (5), test different densities, and study the effect of adding an extra surface term [c.f. Eq. (9)] to the single-folded potential; iv) parametrize the S matrix and study the energy dependence of the "strong-absorption radius" parameter, thus making a link with similar studies performed in the 1980s for heavy-ion reactions [17] and more recently by Gomes and collaborators to study the reduction of reaction cross sections in term of a geometrical parameter [18].

III. ^{9}C -^{9}Be IMAGINARY POTENTIAL

In this section we discuss the details of the ^{9}C -^{9}Be imaginary potentials. As already argued in [2], one characteristic of a double-folded potential with a zero-range interaction is that its radial shape is determined solely by those of the densities used. As such the distinction of surface and volume terms cannot be usually reproduced. In particular their respective contributions, which are strongly energy dependent, as shown by phenomenological potentials, cannot be distinguished. Indeed, Satchler and Love [19], discussing the folding model for ^{9}Be scattering, found evidence of anomalously large deformation and surface effects, which is consistent with the results of [3]. When experimental data are available, this problem is often solved by renormalizing the folded potential so that it would reproduce the data. However dynamical aspects of surface reactions which are typical and very relevant for light nuclei are difficult to reproduce even with a renormalized folded potential. In particular, we notice that the "unphysical" positive imaginary potentials that sometimes have been introduced at short distances, might simply reflect the need to correct the folded potential, which is too attractive in the interior, thus making the resulting potential more surfaced peaked [20,21].

Indeed coupled-channel calculations have overcome such difficulties [22–24].

In the following of the paper we will discuss differences in the imaginary part of two types of potentials: the ^{9}C -^{9}Be potential obtained making a single-folding calculation in which we use one density and the nucleon-nucleus phenomenological potential [3] vs. the double-folded and JLM potentials. The accuracy of such a procedure can be checked by using these potentials to calculate total reaction cross sections and compare them to experimental results. Such cross sections will be calculated, in the eikonal approximation, without renormalizing the potential for all but the JLM case. At energies smaller than about 80 MeV/nucleon, we notice that the loosely bound nature of the projectiles would provide a second-order imaginary term to the potential representing the valence nucleon breakup channels. Since the folding model misses such a term, we have added to the single-folding potential, a surface potential of the Woods-Saxon–derivative type:

$$W(r) = -4a^i W_{\rm surf} \frac{d}{dr} \frac{1}{1+e^{(r-R^i)/a^i}} \tag{9}$$

with very small strength ($W_{\rm surf} = 0.8$ to 0.015 MeV). The radius has been taken [25] as $R^i = 0.92\,(A_p^{1/3} + A_t^{1/3}) = 3.8$ fm, which is close to the distance of closest approach for head on collisions where the absorption is maximized. On the other hand the diffuseness should be large according to [2,25], and equal to $a^i = 1/(2\sqrt{2mS_p}/\hbar) = 2$ fm for ^{9}C, since $S_p = 1.296$ MeV.

A. n-^{9}Be imaginary potential

In Ref. [2] we compared the DOM and AB potentials with the potential from Eq. (6). It was shown that both of these "phenomenological" potentials are shallower in the interior than at the surface, thus having a longer range than the folded potential, although the latter was obtained from a realistic VMC density [4,5]. Therefore this observation clarified that when one such neutron-nucleus potential is then folded with a projectile density, the resulting potential, at least for a light, very deformed nucleus like ^{9}Be, will miss the strong dynamical effect, contained instead in a phenomenological potential, of a surface dominance and a longer range. Besides, it will be affected by the ambiguities discussed in Ref. [26] related to the choice of the nucleon-nucleon cross section.

B. ^{9}C -^{9}Be

In this section, we study a series of potentials and calculate the associated $^9\mathrm{C} + {}^9\mathrm{Be}$ reaction cross sections.

The double folding will be performed with predicted VMC and Hartree-Fock (HF) densities, and with the JLM method. In contrast to this we will single fold the (AB) potential of Ref. [3] with the same VMC and HF densities and compare the results. For comparison we will also consider a relativistic Hartree Fock density [27], the multiple-width Gaussian basis method density based on antisymmetrized molecular dynamics [28] and the microscopic cluster density [29].

Our procedure will suggest ways to determine the "strong-absorption radius" R_s at which $|S_{NN}|^2 = \frac{1}{2}$, and the diffusivity parameter a for a parametrized form of the S matrix, i.e.,

$$S_{NN} = \exp\left(-\ln 2 e^{(R_s-b)/a}\right). \tag{10}$$

Due to the energy dependence of the optical potential, the strong-absorption radius is also energy dependent. It is customary to parametrize such as a dependence as

$$R_s = r_s(E_{\rm inc})\left(A_p^{1/3} + A_t^{1/3}\right). \tag{11}$$

Equation (10) is also used to describe [30] the core-target elastic scattering, or "survival probability" in one-nucleon transfer and/or knockout reactions and thus it constraints the core-target S-matrix S_{ct} which is a very relevant quantity in the calculation of the absolute cross sections and in the extraction of the "experimental" spectroscopic factors.

We start by showing in Figs. 1 and 2 imaginary potentials corresponding to 20, 38, 65, and 83 MeV/nucleon. We show separately the JLM renormalized in order to fit the experimental data, the double-folded potential calculated with

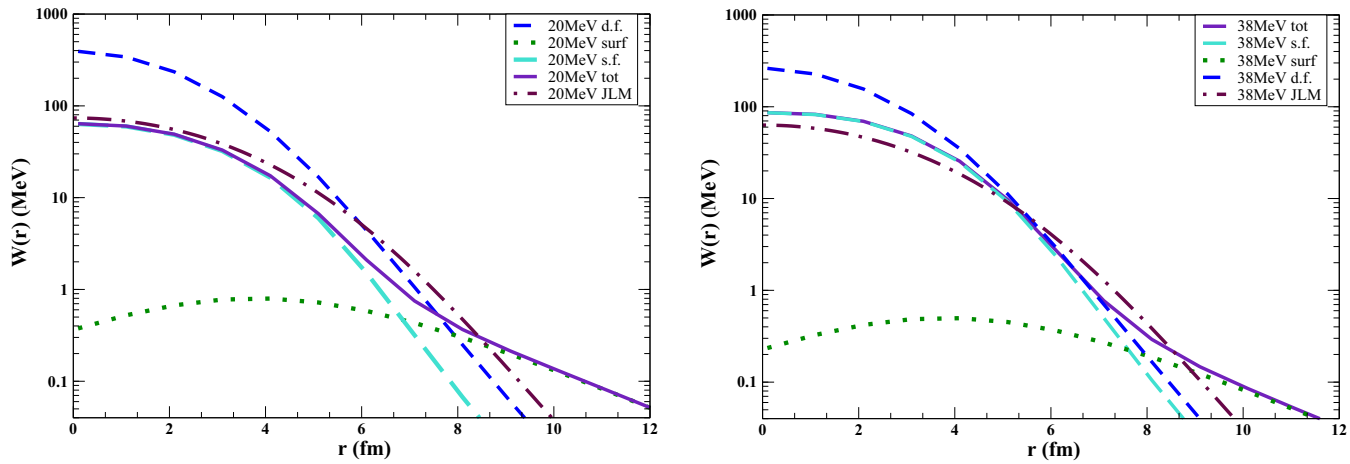

FIG. 1. Potentials calculated at 20 (LHS) and 38 MeV/nucleon (RHS). These include the double-folded (d.f.) and the single-folded (s.f.) results. The surface contribution (surf), the sum of the single-folded and surface values (tot), and the JLM result. The double-folded potentials are calculated with the HF densities.

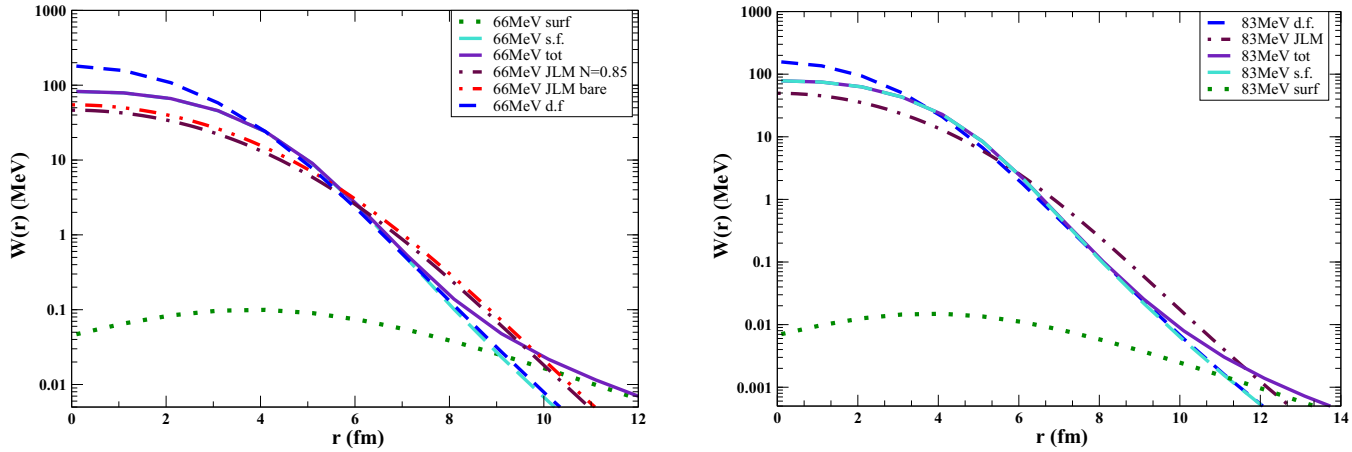

FIG. 2. As for Fig. 1 but now the potentials are calculated at 66 (LHS) and 83 MeV/nucleon (RHS). At 66 MeV/nucleon the "bare" JLM (JLM bare) is also shown.

the HF densities (d.f.), the single-folded potential (s.f.), Eq. (4), obtained also using the HF densities, the surface correction (surf) Eq. (9), and the sum of the two (tot). The strength of a surface potential due to breakup, according to Ref. [25] is very small. Here we have constrained its magnitude in order to get cross sections close to the experimental values. It is clear that the surface correction has the effect of modifying the tail of the potentials and that this tail is more evident at low energies. We interpret this as an effective way of taking into account the "halo" of the ^{9}C projectile and in particular, its breakup. In Table I we give the volume integrals per number of interacting nucleon pairs of these potentials, their rms radius, and the strength of the surface term Eq. (9). The volume integral and rms radius calculated with the VMC densities is also given for comparison although this potential is not shown in the previous figures. Obviously the volume integrals of the double-folded potentials are the same because all densities are normalized to the correct number of neutron and protons in the projectile and target. Thus the volume integrals depend only on the velocity of relative motion and the free $\sigma_{np,pp}$ which we take from the parametrization given in Ref. [26]. The rms radii are however different because the VMC and HF densities have different rms radii whose values are given on Fig. 4.

Then in Table II for a series of incident energies of the system ^{9}C + ^{9}Be, we give in the second column some data from Ref. [32]; in columns three and four, the calculated total reaction cross sections with the double-folded potential in two cases. One with ^{9}C and ^{9}Be densities from VMC; the other with both densities from HF. In the next columns we provide cross section obtained by single-folding the (AB) potential from Ref. [3] with a HF density for ^{9}C and then adding the surface potential Eq. (9) whose strength is also given, the "bare" JLM results and those with the "renormalized" JLM are also shown as indicated. The renormalization factor is given in the next column. For the single-folded-plus-surface calculation, we provide then the strong-absorption radius and diffuseness a obtained from a fit to the calculated $|S_{NN}|^2$ with Eq. (10). Other projectile densities have also been tested [4,27–29] in the single-folding formula Eq. (4) and the dependence of the cross sections on the density used is shown of the (LHS) of Fig. 3. The long-dashed curve is from the microscopic cluster model density [29]; short dashed curve is from the molecular dynamics density [28]; dotted-dashed curve is from HF density and double-dotted-dashed curve is from VMC density [4]; double-dashed-dotted curve is the "bare" JLM result. The relativistic HF density [27] gives results very close to HF and it is not shown for simplicity. Furthermore the full curves correspond to the calculations with the double-folded potentials. Thick curves obtained with HF densities, while thin curves obtained with VMC densities. These two calculations show a behavior with energy similar to the data, but as expected [31] the absolute values are smaller than the data [32]. The single folded potentials with VMC and HF densities give a good reproduction of both the energy dependence and the magnitude of the data, but only at energies higher than about 60 MeV/nucleon. Figure 4 shows the densities we have used. In the inset, they are reported on a logarithm scale to visualize their different tails at large radii. Part of the reason for the small

TABLE I. Volume integrals of the imaginary potentials shown in Figs. 1, 2, their rms radii, and the strength of the surface term $W_{\rm surf}$ (see text).

$E_{\rm lab}$ (MeV/nucleon)	$J_{\rm d.f.VMC}$ (MeV fm^3)	rms (fm)	$J_{\rm d.f.HF}$ (MeV fm^3)	rms (fm)	$J^{\rm ren}_{\rm JLM}$ (MeV fm^3)	rms (fm)	$J^{+\rm surf}_{\rm s.fold}$ (MeV fm^3)	rms (fm)	$J_{\rm s.fold}$ (MeV fm^3)	rms (fm)	$W_{\rm surf}$ (MeV)
20	657	3.38	656	3.55	259	4.42	198	4.72	172	3.81	0.8
38	438	3.38	437	3.55	212	4.40	272	4.29	255	3.85	0.5
66	302	3.38	301	3.55	143	4.31	248	3.96	245	3.86	0.1
83	262	3.38	261	3.55	147	4.27	232.2	3.87	231.7	3.85	0.015

TABLE II. Experimental reaction cross sections, second column, from Ref. [32]. Calculated total reaction cross sections with the double-folded potential using VMC densities for both ^{9}C and ^{9}Be (third column); double-folded potential using HF densities for both ^{9}C and ^{9}Be (fourth column); using the single-folded potential with HF density for ^{9}C (fifth column) and with the added surface potential (sixth column), with the "bare" JLM and with the renormalized JLM for $^9\mathrm{C}+{}^9\mathrm{Be}$. The renormalization factor for the JLM potential and strength of the additional surface potential for the single-folded potential are also given. For the case of $\sigma_{\mathrm{s.fold}}^{+\mathrm{surf}}$ we then give strong-absorption radius R_s from $|S_{NN}(R_s)|^2 = \frac{1}{2}$, and R_S^{fit} from the fit to the calculated $|S_{NN}|^2$ according to Eq. (10). In this case also the diffuseness-like parameter is given. Last column: r_s from Eq. (11) and R_s.

E_{lab} (MeV/nucleon)	σ_{exp} (mb)	$\sigma_{\mathrm{d.fold}}^{\mathrm{VMC}}$ (mb)	$\sigma_{\mathrm{d.fold}}^{\mathrm{HF}}$ (mb)	$\sigma_{\mathrm{s.fold}}$ (mb)	$\sigma_{\mathrm{s.fold}}^{+\mathrm{surf}}$ (mb)	$\sigma_{\mathrm{JLM}}^{\mathrm{bare}}$ (mb)	$\sigma_{\mathrm{JLM}}^{\mathrm{ren}}$ (mb)	N_{JLM}	$\mathrm{W}_{\mathrm{surf}}$ (MeV)	R_s (fm)	R_s^{fit} (fm)	a^{fit} (fm)	r_s (fm)
20		1267	1409	1078	1565	1338	1538	1.65	0.8	6.12	6.25	1.01	1.47
38		1086	1191	1112	1341	1250	1324	1.20	0.5	5.95	5.99	0.97	1.44
40.9	1216 ± 57	1064	1166	1117	1291	1235	1215	0.95	0.4	5.95	5.99	0.98	1.44
43		1050	1148	1103	1275	1221	1260	1.10	0.4	5.95	5.99	0.99	1.44
43.6	1269 ± 22	1046	1144	1106	1235	1219	1257	1.10	0.3	5.82	5.70	0.80	1.40
59		960	1042	1047	1124	1130	1111	0.95	0.2	5.70	5.64	0.82	1.36
61.1	1104 ± 20	950	1030	1045	1122	1119	1119	1.00	0.2	5.68	5.63	0.83	1.36
66		928	1006	1028	1066	1091	1028	0.85	0.1	5.60	5.55	0.80	1.35
67.4	1074 ± 32	923	999	1026	1056	1087	1087	1.00	0.08	5.60	5.53	0.80	1.35
68.3	1064 ± 16	919	995	1024	1052	1082	1063	0.95	0.075	5.55	5.49	0.80	1.33
83		867	934	948	979	1015	987	0.93	0.015	5.40	5.38	0.78	1.29
84.9	981 ± 15	861	928	979	983	1008	989	0.95	0.01	5.40	5.36	0.80	1.29
95		833	895	949	952	968	956	0.97	0.01	5.40	5.28	0.79	1.29
97.2	919 ± 24	827	888	949	951	963	923	0.90	0.005	5.35	5.28	0.80	1.28

cross sections obtained with these model densities is that they do not extend to large enough radii. Notice that from about 5 fm the various densities show differences on a logarithmic scale. Here they have already dropped by three orders of magnitude with respect to the central density. Still the corresponding total reaction cross sections, Fig. 3 (LHS) show differences thus suggesting once again the very-long-range nature of the nuclear interaction for halo nuclei. Finally on the right-hand side of Fig. 3 we report again the data [32] together with our results from the single folding with HF density plus the surface term (full cyan line) and the renormalized JLM (dot-dashes brown line). Both calculations reproduce the energy slope and the absolute values of the data. We report for completeness also the experimental values [33,34] and theoretical cross sections [2] for ^{8}Li and ^{8}B projectiles. Note the very close similarity between the ^{8}B and ^{9}C values.

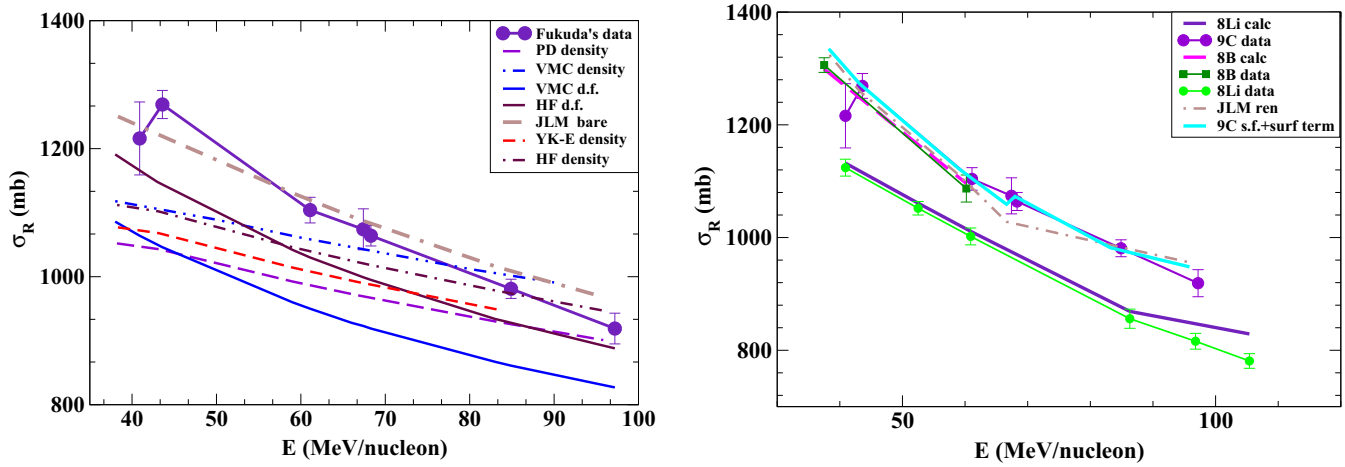

FIG. 3. (LHS) Energy dependence of the reaction cross sections for ^{9}C -^{9}Be calculated according to Eq. (1). We compare results obtained using the the single-folding potential with n-^{9}Be from [3] and various projectile densities, in particular VMC [4], YK-E [28], PD [29] (see also text), and JLM. The two full lines are the results of calculations with the double-folded potentials. Thick maroon line is with HF densities, blue thin line with VMC densities. Data are from Ref. [32]. (RHS) We show here again the data from Ref. [32] and results of reaction cross section calculations which have been modified to fit the data. One is from the single-folding potential plus the additional surface term Eq. (9), the second is a renormalized JLM. For comparison results obtained for ^{8}Li and ^{8}B projectiles from Ref. [2] using the single-folded plus surface term potential. Data are from Refs. [33,34].

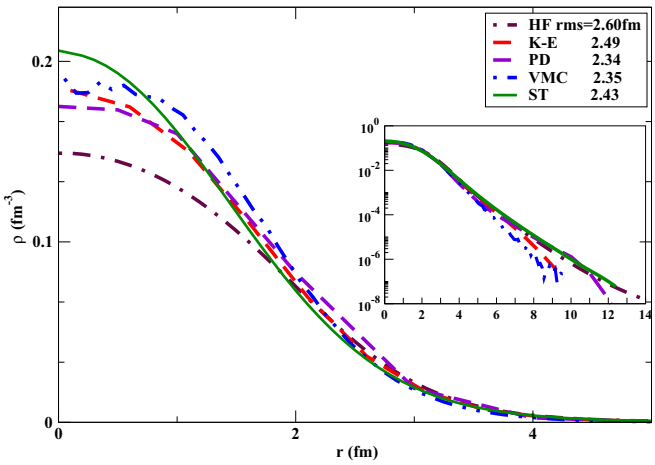

FIG. 4. ^{9}C densities used in the calculated cross sections shown in Fig. 2.

One interesting result of our study, as seen in Table I, is that although the volume integrals of the potentials obtained by double-folding VMC and HF densities are basically identical, their radii are not. The potentials obtained with HF densities have slightly larger radii and this reflects in the larger cross sections shown in Table II. This finding is intriguing and contradicts the common wisdom that potentials with equal volume integrals would give equal reaction cross sections. We believe this situation is novel in what we are dealing with very-light and deformed nuclei in which the surface and surface-dominated reactions must be dominant over volume characteristics. Furthermore we notice that the JLM potential, even in the bare case, provides cross sections larger than the two double-folded potentials although its volume integrals are much smaller. Once again, this is due to the fact that its radii are larger than those of the double-folded potentials. In fact the HF densities we have used for JLM were obtained from a HF calculation in which the surface term of the density functional was adjusted to reproduce the experimental binding energy. With this procedure the single particle levels near the Fermi energy are more realistic and the resulted range reflects in some measure the delocalization of the weakly bound neutrons. However our goal here is to obtain the best absolute cross sections at all energies. This does not seem possible by using any of the projectile densities we have tried. Indeed, as it is shown by Fig. 3 (LHS), the slope does not depend on the density.

In Fig. 5 we show the S matrices (LHS) at 66 MeV/nucleon and the total integrand of Eq. (1) (RHS). One notices that the JLM potential gives the largest cross sections because the S matrix attains the unitary value at larger distances than with the other potentials. The large impact parameters contribute indeed mostly to the reaction cross section. This can be understood by looking at the JLM potential shown in Fig. 2 (RHS). Overall, this potential is not as deep as the other potentials but it has a region on the surface (between about 5 fm to 10 fm) where it is deeper than all other potentials. On the other hand we notice that the double-folded potential gives rise to a "sharper" S matrix, corresponding also to a smaller strong-absorption radius. As we anticipated, this is because the important surface effects are missing.

Looking again at Fig. 3, we notice that the simple addition of the very weak surface potential to the single-folded potential provides the change of slope in the energy dependence of the reaction cross section, expected on the basis of the published experimental results of similar systems [2,33,34]. Furthermore we notice from Table II that the strength of the extra surface term has dropped by two orders of magnitude from 80 MeV/nucleon on and indeed the results look independent from the presence of the extra surface imaginary potential. Consistent with our expectations, this result shows that at high energies the imaginary potential is of volume type and that its strength has saturated. Thus it appears that the energy dependence of the n-^{9}Be potential [3] is enough to provide the correct energy dependence of the nucleus-^{9}Be potential for energies larger than about 65 MeV/nucleon, and the single-folded potential as given by Eq. (4) will then have an accurate predictive power without any correction or renormalization.

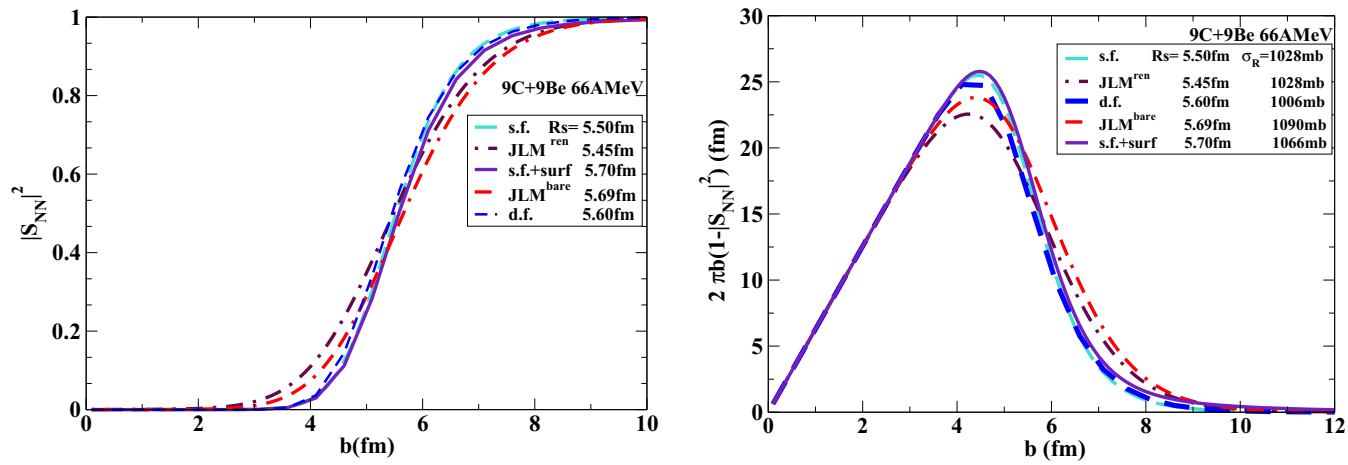

FIG. 5. (LHS) S matrices calculated at 66 MeV/nucleon with the potentials indicated in the legend. (RHS) Integrand in Eq. (1). See text for details.

IV. CONCLUSIONS

As we mentioned in the Introduction and shown by our calculations, double-folded potentials are unable to reproduce experimental reaction cross sections, irrespective of the densities used. Several ad hoc corrections have been applied in the literature [20–24]. In order to minimize such corrections and obtain also a better understanding of the reaction channels contributing to the reaction cross section, we have presented in this work, some results obtained using new ideas to improve the understanding and calculations of the nucleus-nucleus imaginary potential for scattering of exotic light nuclei, the corresponding S matrices and total reaction cross sections. We have been concerned with systems like ^{9}C -^{9}Be for which the optical potential and, in particular, the double-folded-model version of it needs careful handling and a good understanding of the reaction channels involved. The existing formalisms, such as for example JLM, have been improved because no arbitrary renormalization has been applied to the folded potential. This has been done using a single-folding model in which the n-^{9}Be target potential has been taken from a phenomenological fit to data over a large range of energies [3]. Projectile densities have been taken from a series of microscopic calculations [4,5,27–29] and results have been compared. Depending on the projectile density used, the absolute cross sections are different but the slope of the energy dependence of the cross section is the same. Because it appears that none of those distributions is able to describe the low-energy increase of the reaction cross sections, a semimicroscopic surface term has been included according to Ref. [25]. Such a term has the diffuseness obtained from the projectile valence particle separation energy while the strength is very small. It is clear that a potential of this type does not modify the internal absorption but simply reproduces surface reactions such as breakup which are important for weakly bound nuclei. Thus it cannot be considered as a renormalization of the whole potential because it modifies only its tail. The results are extremely encouraging and we propose that by using n,p-target phenomenological potentials fitted to experimental data, folded with exotic nuclei densities, reaction cross sections could be calculated and compared to experimental data. Missing surface effects could be reproduced adding surface potentials according to Ref. [25].

ACKNOWLEDGMENTS

We are grateful to Yoshiko Kanada En'yo, Pierre Descouvemont, Stefan Typel, and Bob Wiringa for providing their numerical densities and for discussions and to M. Fukuda and D. Nishimura for providing their experimental data values. F.C. was partially supported by INFN-Pisa and CNCSIS (Romania) PN II 55/2011. R.J.C. was funded by the U.S. Department of Energy, Office of Science, Office of Nuclear Phyics under Award No. DE-FG02-87ER-40316.

[1] I. Tanihata, J. Phys. G. **22**, 157 (1996).
[2] A. Bonaccorso, F. Carstoiu, R. J. Charity, R. Kumar, and G. Salvioni, Few-Body Syst. **57**, 331 (2016).
[3] A. Bonaccorso and R. J. Charity, Phys. Rev. C **89**, 024619 (2014).
[4] R. B. Wiringa, http://www.phy.anl.gov/theory/research/density/.
[5] S. C. Pieper and R. B. Wiringa, Annu. Rev. Nucl. Part. Sci. **51**, 53 (2001).
[6] J. P. Jeukenne, A. Lejeune, and C. Mahaux, Phys. Rev. C **16**, 80 (1977).
[7] F. Duggan, M. Lassaut, F. Michel, and N. Vinh Mau, Nucl. Phys. A **355**, 141 (1981).
[8] L. Trache, A. Azhari, H. L. Clark, C. A. Gagliardi, Y.-W. Lui, A. M. Mukhamedzhanov, R. E. Tribble, and F. Carstoiu, Phys. Rev. C **61**, 024612 (2000).
[9] A. Bonaccorso and F. Carstoiu, Phis. Rev. C **61**, 034605 (2000).
[10] T. Motobayashi, Nucl. Phys. A **718**, 101c (2003); private communication.
[11] R. J. Charity *et al.*, Phys. Rev. C **84**, 014320 (2011).
[12] M. F. Jager *et al.*, Phys. Rev. C **86**, 011304(R) (2012).
[13] I. A. Egorova *et al.*, Phys. Rev. Lett. **109**, 202502 (2012).
[14] K. W. Brown *et al.*, Phys. Rev. Lett. **113**, 232501 (2014).
[15] D. Gogny, in *Proceedings of the International Conference on Nuclear Physics, Munich*, edited by J. de Boer and H. J. Mang (North Holland Publishing Company, Amsterdam, London; American Elsevier Publishing Company, INC-New York, 1973), p. 48.
[16] N. Anantaraman, H. Toki, and G. F. Bertsch, Nucl. Phys. A **398**, 269 (1983).
[17] R. Bass, *Nuclear Reactions with Heavy Ions* (Springer-Verlag, Berlin/Heidelberg/New York, 1980), Sec. 3.3.
[18] L. F. Canto, D. R. Mendes Junior, P. R. S. Gomes, and J. Lubian, Phys. Rev. C **92**, 014626 (2015).
[19] G. R. Satchler and W. G. Love, Phys. Rep. **55**, 183 (1979).
[20] M. Aygun, I. Boztosun, and K. Rusek, Mod. Phys. Lett. A **28**, 1350112 (2013)
[21] V. Lapoux *et al.*, Phys. Lett. B **658**, 198 (2008), and references therein.
[22] Y. Sakuragi, Phys. Rev. C **35**, 2161 (1987).
[23] V. Lapouxa and N. Alamanos, Eur. Phys. J. A **51**, 91 (2015).
[24] N. Keeley, K. W. Kemper, and K. Rusek, Eur. Phys. J. A **50**, 145 (2014).
[25] A. Bonaccorso and F. Carstoiu, Nucl. Phys. A **706**, 322 (2002).
[26] C. A. Bertulani and C. De Conti, Phys. Rev. C **81**, 064603 (2010).
[27] S. Typel, G. Röpke, T. Klahn, D. Blaschke, and H. H. Wolter, Phys. Rev. C **81**, 015803 (2010).
[28] N. Furutachi, M. Kimura, A. Doté, and Y. Kanada-En'yo, Prog. Theor. Phys. **122**, 865 (2009).
[29] P. Descouvement, Nucl. Phys. A **646**, 261 (1999).
[30] A. Bonaccorso, D. M. Brink, and L. Lo Monaco, J. Phys. G **13**, 1407 (1987).
[31] A. Ozawa *et al.*, Nucl. Phys. A **691**, 599 (2001); A. Ozawa, AIP Conf. Proc. **865**, 57 (2006).

[32] M. Fukuda *et al.*, private communication; D. Nishimura *et al.*, Osaka University Laboratory of Nuclear Studies (OULNS) Annual Report 2006, p. 37.
[33] G. W. Fan, M. Fukuda, D. Nishimura, X. L. Cai, S. Fukuda, I. Hachiuma, C. Ichikawa, T. Izumikawa, M. Kanazawa, A. Kitagawa, T. Kuboki, M. Lantz, M. Mihara, M. Nagashima, K. Namihira, Y. Ohkuma, T. Ohtsubo, Z. Ren, S. Sato, Z. Q. Shen, M. Sugiyama, S. Suzuki, T. Suzuki, M. Takechi, T. Yamaguchi, B. J. Xu, and W. Xu, Phys. Rev. C **90**, 044321 (2014).
[34] M. Fukuda *et al.*, Nucl. Phys. A **656**, 209 (1999).